

Precision Measurements of A_1^n in Deep Inelastic Regime
v 1.1, 24 February 2014 – for internal E06-014 distribution only

D. S. Parno,^{1,2,*} D. Flay,³ M. Posik,³ K. Allada,⁴ W. Armstrong,³ T. Averett,⁵ F. Benmokhtar,¹ W. Bertozzi,⁶
A. Camsonne,⁷ M. Canan,⁸ G.D. Cates,⁹ C. Chen,¹⁰ J.-P. Chen,⁷ S. Choi,¹¹ E. Chudakov,⁷ F. Cusanno,^{12,13}
M. M. Dalton,⁹ W. Deconinck,⁶ C.W. de Jager,⁷ X. Deng,⁹ A. Deur,⁷ C. Dutta,⁴ L. El Fassi,¹⁴ G. B. Franklin,¹
M. Friend,¹ H. Gao,¹⁵ F. Garibaldi,¹² S. Gilad,⁶ R. Gilman,^{7,14} O. Glamazdin,¹⁶ S. Golge,⁸ J. Gomez,⁷
L. Guo,¹⁷ O. Hansen,⁷ D. W. Higinbotham,⁷ T. Holmstrom,¹⁸ J. Huang,⁶ C. Hyde,^{8,19} H. F. Ibrahim,²⁰
X. Jiang,^{14,17} G. Jin,⁹ J. Katich,⁵ A. Kelleher,⁵ A. Kolarkar,⁴ W. Korsch,⁴ G. Kumbartzki,¹⁴ J.J. LeRose,⁷
R. Lindgren,⁹ N. Liyanage,⁹ E. Long,²¹ A. Lukhanin,³ V. Mamyas,¹ D. McNulty,²² Z.-E. Meziani,³ R. Michaels,⁷
M. Mihovilović,²³ B. Moffit,^{6,7} N. Muangma,⁶ S. Nanda,⁷ A. Narayan,²⁴ V. Nelyubin,⁹ B. Norum,⁹
Nuruzzaman,²⁴ Y. Oh,²⁵ J. C. Peng,²⁶ X. Qian,^{15,27} Y. Qiang,^{15,7} A. Rakhman,²⁸ R. D. Ransome,¹⁴
S. Riordan,⁹ A. Saha,^{7,†} B. Sawatzky,^{3,7} M. H. Shabestari,⁹ A. Shahinyan,²⁹ S. Širca,³⁰ P. Solvignon,^{31,7}
R. Subedi,⁹ V. Sulkosky,^{6,7} A. Tobias,⁹ W. Troth,¹⁸ D. Wang,⁹ Y. Wang,²⁶ B. Wojtsekhowski,⁷ X. Yan,³²
H. Yao,^{3,5} Y. Ye,³² Z. Ye,¹⁰ L. Yuan,¹⁰ X. Zhan,⁶ Y. Zhang,³³ Y.-W. Zhang,^{33,14} B. Zhao,⁵ and X. Zheng⁹

(The Jefferson Lab Hall A Collaboration)

¹*Carnegie Mellon University, Pittsburgh, PA 15213*

²*Center for Experimental Nuclear Physics and Astrophysics, University of Washington, Seattle, WA 98195*

³*Temple University, Philadelphia, PA 19122*

⁴*University of Kentucky, Lexington, KY 40506*

⁵*College of William and Mary, Williamsburg, VA 23187*

⁶*Massachusetts Institute of Technology, Cambridge, MA 02139*

⁷*Thomas Jefferson National Accelerator Facility, Newport News, VA 23606*

⁸*Old Dominion University, Norfolk, VA 23529*

⁹*University of Virginia, Charlottesville, VA 22904*

¹⁰*Hampton University, Hampton, VA 23187*

¹¹*Seoul National University, Seoul, South Korea*

¹²*INFN, Sezione di Roma, I-00161 Rome, Italy*

¹³*Istituto Superiore di Sanità, I-00161 Rome, Italy*

¹⁴*Rutgers, The State University of New Jersey, Piscataway, NJ 08855*

¹⁵*Duke University, Durham, NC 27708*

¹⁶*Kharkov Institute of Physics and Technology, Kharkov 61108, Ukraine*

¹⁷*Los Alamos National Laboratory, Los Alamos, NM 87545*

¹⁸*Longwood University, Farmville, VA 23909*

¹⁹*Université Blaise Pascal/IN2P3, F-63177 Aubière, France*

²⁰*Cairo University, Giza 12613, Egypt*

²¹*Kent State University, Kent, OH 44242*

²²*University of Massachusetts, Amherst, MA 01003*

²³*Jožef Stefan Institute, Ljubljana, Slovenia*

²⁴*Mississippi State University, MS 39762*

²⁵*Kyungpook National University, Taegu 702-701, Republic of Korea*

²⁶*University of Illinois at Urbana-Champaign, Urbana, IL 61801*

²⁷*Kellogg Radiation Laboratory, California Institute of Technology, Pasadena, Ca 91125*

²⁸*Syracuse University, Syracuse, NY 13244*

²⁹*Yerevan Physics Institute, Yerevan 375036, Armenia*

³⁰*University of Ljubljana, SI-1000 Ljubljana, Slovenia*

³¹*Argonne National Lab, Argonne, IL 60439*

³²*University of Science and Technology of China, Hefei 230026, People's Republic of China*

³³*Lanzhou University, Lanzhou 730000, Gansu, People's Republic of China*

(Dated: February 24, 2014)

We have performed precision measurements of the double-spin virtual photon-neutron asymmetry A_1^n in the deep inelastic scattering regime, over a wide kinematic range $0.277 \leq x \leq 0.548$ and at an average Q^2 value of 2.89 (GeV/c)^2 , demonstrating competitive uncertainties and good control over background in an open-geometry, large-acceptance spectrometer. Our measurement doubles the available high-precision neutron data in this x range. We have combined our results with world data on proton targets to extract the ratio of polarized-to-unpolarized parton distribution functions for up quarks and for down quarks in the same kinematic range. Our data corroborate the previous observation of an A_1^n zero crossing near $x = 0.5$. We also confirm that $(\Delta d + \Delta \bar{d})/(d + \bar{d}) \leq 0$ in the measured x range, in contrast to predictions of leading-order perturbative quantum chromodynamics

without orbital angular momentum.

PACS numbers: 14.20.Dh, 24.85.+p, 25.30.-c

Ever since the European Muon Collaboration determined that the quark-spin contribution was insufficient to account for the spin of the proton [1], the origin of the nucleon spin has been an open puzzle; see [2] for a recent review. While recent preliminary results suggest a non-zero contribution from the gluon spin [3], the role of parton orbital angular momentum is also under investigation. In the valence quark region, combining spin-structure data on protons and neutrons allows the separation of contributions from up and down quarks and permits a sensitive test of several theoretical models.

In deep inelastic scattering (DIS), nucleon structure is conventionally parameterized by the unpolarized structure functions $F_1(x, Q^2)$ and $F_2(x, Q^2)$, and by the polarized structure functions $g_1(x, Q^2)$ and $g_2(x, Q^2)$, where Q^2 is the negative square of the four-momentum transferred in the scattering interaction and x is the Bjorken scaling variable, which in the infinite-momentum frame is equal to the fraction of the nucleon momentum carried by the struck quark. The virtual photon-nucleon asymmetry A_1 probes the nucleon spin structure. Where $\sigma_{1/2(3/2)}$ is the cross section of virtual photoabsorption on the nucleon for a total spin projection of $1/2$ ($3/2$) along the virtual-photon momentum direction, $A_1 = (\sigma_{1/2} - \sigma_{3/2})/(\sigma_{1/2} + \sigma_{3/2})$. At finite Q^2 , this asymmetry may be expressed in terms of the nucleon structure functions as

$$A_1(x, Q^2) = [g_1(x, Q^2) - \gamma^2 g_2(x, Q^2)] / F_1(x, Q^2), \quad (1)$$

where $\gamma^2 = 4M^2 x^2 / Q^2$ and M is the nucleon mass. For large Q^2 , $\gamma^2 \ll 1$ and $A_1(x) \approx g_1(x) / F_1(x)$; since g_1 and F_1 have the same Q^2 evolution to leading order, A_1 may be approximated as a function of x alone. Through Eq. 1, A_1 also gives access to the unpolarized and polarized parton distribution functions (PDFs) $q(x) = q^\uparrow(x) + q^\downarrow(x)$ and $\Delta q(x) = q^\uparrow(x) - q^\downarrow(x)$, where $q^{\uparrow(\downarrow)}$ is the probability of finding the quark q with a given value of x and with spin (anti)parallel to that of the nucleon.

The close connection of A_1 to the nucleon structure functions has inspired its calculation in a wide variety of models, several of which are represented in Fig. 1. Most of these models predict that $A_1^{n,p} \rightarrow 1$ as $x \rightarrow 1$. Calculations in the relativistic constituent quark model (RCQM), for example, generally assume that SU(6) symmetry is broken via a color hyperfine interaction between quarks, lowering the energy of spectator-quark pairs in a spin singlet state relative to those in a spin triplet state and increasing the probability that, at high x , the struck quark carries the nucleon spin [4]. In perturbative quantum chromodynamics (pQCD), valid at large x and

large Q^2 where the coupling of gluons to the struck quark is small, the leading-order assumption that the valence quarks have no orbital angular momentum leads to the same conclusion about the spin of the struck quark [5, 6]. Parameterizations of the world data, in the context of pQCD models, have been made both with and without this assumption of hadron helicity conservation. The LSS(BBS) parameterization [7] is a classic example of the former; more recently, a parameterization by Avakian *et al.* [8] explicitly includes Fock states with nonzero quark orbital angular momentum.

The statistical model treats the nucleon as a gas of massless partons at thermal equilibrium, using both chirality and DIS data to constrain the thermodynamical potential of each parton species. At a moderate Q^2 value of 4 (GeV/c)², $A_1^{n,p} \rightarrow 0.6\Delta u(x)/u(x)$ as $x \rightarrow 1$ [9]. Statistical-model predictions are thus in conflict with RCQM and pQCD for finite values of Q^2 , unless a positivity violation is permitted.

Recently, Roberts, Holt and Schmidt [10] have explored an approach based on Dyson-Schwinger equations (DSE), in which a baryon is described according to the relevant Poincaré-covariant Faddeev equation with the useful simplification that the sum of soft, dynamical, non-pointlike diquark correlations approximates the quark-quark scattering matrix. $A_1^n(x = 1)$ is predicted at 0.34 in a contact-interaction framework, in which the dressed light-quark mass is taken as a constant 0.4 GeV/c², and at 0.17 in a more realistic framework in which the dressed-quark mass is permitted to depend on momentum. Both predictions are significantly smaller than even the statistical prediction at $x = 1$. However, existing DIS data do not extend to high enough x to definitively favor one model over another.

The virtual photon-nucleon asymmetry A_1 can be extracted from measured electron-nucleon asymmetries. With the beam and target both polarized longitudinally with respect to the beamline, $A_{||} = (\sigma^{\downarrow\uparrow} - \sigma^{\uparrow\uparrow})/(\sigma^{\downarrow\uparrow} + \sigma^{\uparrow\uparrow})$ is the scattering asymmetry between configurations with the electron spin anti-aligned (\downarrow) and aligned (\uparrow) with the beam direction. Meanwhile, $A_{\perp} = (\sigma^{\downarrow\rightarrow} - \sigma^{\uparrow\rightarrow})/(\sigma^{\downarrow\rightarrow} + \sigma^{\uparrow\rightarrow})$ is measured with the target spin perpendicular to the beam direction, pointing to the side on which scattered electrons are detected. A_1 may be related to these asymmetries through [11]:

$$A_1 = \frac{1}{D(1+\eta\xi)} A_{||} - \frac{\eta}{d(1+\eta\xi)} A_{\perp}, \quad (2)$$

where the kinematic variables are given in the laboratory frame by $D = (E - \epsilon E')/(E(1 + \epsilon R))$, $\eta = \epsilon\sqrt{Q^2}/(E - \epsilon E')$, $d = D\sqrt{2\epsilon}/(1 + \epsilon)$, and $\xi = \eta(1 + \epsilon)/2\epsilon$.

Here, E is the initial electron energy; E' is the scattered electron energy; $\epsilon = 1/[1 + 2(1 + 1/\gamma^2) \tan^2(\theta/2)]$; θ is the electron scattering angle; and $R = \sigma_L/\sigma_T$, parameterized via R1998 [12], is the ratio of the longitudinal to the transverse virtual photoabsorption cross sections.

Experiment E06-014 ran in Hall A of Jefferson Lab in February and March 2009. Longitudinally polarized electrons were generated via illumination of a strained superlattice GaAs photocathode by circularly polarized laser light [13] and delivered to the experimental hall with energies of 4.7 and 5.9 GeV. The rastered 12–15- μ A beam was incident on a target of ^3He gas, polarized in the longitudinal and transverse directions via spin-exchange optical pumping of an Rb-K mixture [14] and contained in a 40-cm-long glass cell. The left high-resolution spectrometer [15] and BigBite spectrometer [16] detected scattered electrons in singles mode at angles of 45° on beam left and right, respectively.

Data for the asymmetry measurements were taken with the BigBite detector stack, which in this configuration included eighteen wire planes in three orientations, a gas Čerenkov detector [17], a pre-shower + shower calorimeter, and a scintillator plane between the calorimeter layers. The primary trigger was formed when signals above threshold were registered in geometrically overlapping regions of the gas Čerenkov and calorimeter. With an angular acceptance of 65 msr, BigBite continuously measured electrons over the entire kinematic range of the experiment, and the sample was later divided into x bins of equal size.

The longitudinal beam polarization was monitored continuously by Compton polarimetry [18, 19] and intermittently by Møller polarimetry [20]. In three run periods with polarized beam, the longitudinal beam polarization P_b averaged 0.74 ± 0.01 ($E = 5.9$ GeV), 0.79 ± 0.01 ($E = 5.9$ GeV), and 0.63 ± 0.01 ($E = 4.7$ GeV). A feedback loop limited the charge asymmetry to within 200 ppm. The target polarization P_t , averaging about 50%, was measured periodically using nuclear magnetic resonance [21] and calibrated with electron paramagnetic resonance; in the longitudinal orientation, the calibration was cross-checked with nuclear magnetic resonance data from a well-understood water target.

The raw asymmetry $A_{||,\perp}^{\text{raw}}$ is corrected for beam and target effects according to $A_{||,\perp}^{\text{cor}} = A_{||,\perp}^{\text{raw}}/(P_b P_t f_{N_2})$, where the dilution factor f_{N_2} , determined from dedicated measurements with an N_2 target, corrects for scattering from the small amount of N_2 gas added to the ^3He target to reduce depolarization effects [22]. An additional kinematic factor of $1/\cos\phi$, where ϕ is the vertical scattering angle, is applied to A_{\perp}^{cor} .

Pair-produced electrons, originating from π^0 decay, contaminate the sample of DIS electrons, especially in the lowest x bins. We measured the yield of this process by reversing the spectrometer polarity to observe e^+ with the same acceptance. Gaps in the kinematic

coverage of these special measurements were filled with data from the left high-resolution spectrometer and with CLAS EG1b [23] data taken at a similar scattering angle. The resulting ratio $f_{e^+} = N_{e^+}/N_{e^-}$ quantifies the contamination of the electron sample with pair-produced electrons. The underlying double-spin asymmetry A^{e^+} of the π^0 production process was measured to be 1–2% using the positron sample obtained during normal BigBite running, and cross-checked against the reversed-polarity positron asymmetry for the available kinematics.

The contamination of the scattered-electron sample with π^- was below 3% in all x bins, limited primarily by the efficiency of the gas Čerenkov in eliminating pions from the online trigger. Due to the low contamination level, the asymmetry in pion production had a negligible ($\lesssim 1\%$) effect on $A_{||}$ and A_{\perp} , and the pion correction to the asymmetry was therefore treated as a pure dilution f_{π^-} . Contamination of the positron sample with π^+ resulted in the dilution factor f_{π^+} .

The final physics asymmetries $A_{||,\perp}$ include internal and external radiative corrections $\Delta A_{||,\perp}^{RC}$ as well as background corrections:

$$A_{||,\perp} = \frac{A_{||,\perp}^{\text{cor}} - f_{e^+} A_{||,\perp}^{e^+}}{1 - f_{\pi^-} - f_{e^+} + f_{\pi^+} f_{e^+}} + \Delta A_{||,\perp}^{RC}. \quad (3)$$

To compute $\Delta A_{||,\perp}^{RC}$, the asymmetries were reformulated as polarized cross-section differences using the F1F209 [24] parameterization for the radiated unpolarized cross section. The polarized elastic tail was computed [25] and found to be negligible in both the parallel and perpendicular cases, and was not subtracted. Radiative corrections were then applied iteratively, according to the formalisms first described by Mo and Tsai [26] for the unpolarized case, and by Akushevich et al. [27] for the polarized case. The DSSV model [28] was used as an input for the DIS region, and the integration phase space was completed in the resonance region with the MAID model [29], and in the quasi-elastic region with the Bosted nucleon form factors [30] smeared with a scaling function [31]. The final results were then converted back to asymmetries. The error on $\Delta A_{||,\perp}^{RC}$ was estimated at $\lesssim 5.2\%$, dominated by model dependence, by varying material thicknesses and input spectra over a range of $\pm 10\%$ and comparing the final results.

Polarized ^3He targets are commonly used as effective polarized neutron targets because, in the dominant S state, the spin of the ^3He nucleus is carried by the neutron. To extract the neutron asymmetry A_1^n from the measured asymmetry $A_1^{^3\text{He}}$ on the nuclear target, we used a model for the ^3He wavefunction incorporating S , S' , and D states as well as a pre-existing $\Delta(1232)$ component [32]:

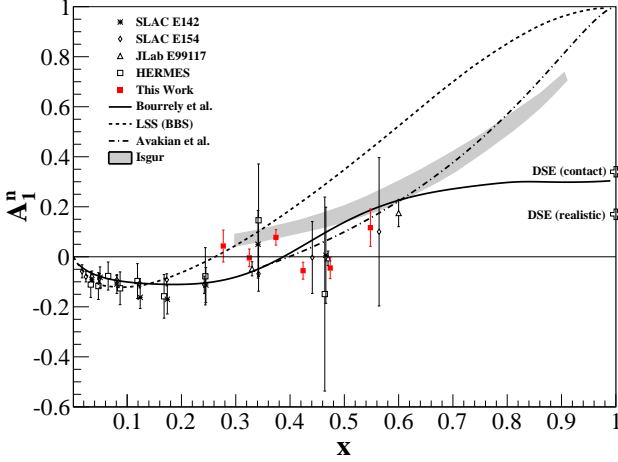


FIG. 1. Our A_1^n results in the DIS regime (red squares), compared with world A_1^n data extracted using ^3He targets (SLAC E142 [40], SLAC E154 [41], JLab E99117 [33], and HERMES [37]). Selected model predictions are also shown: RCQM [4], statistical [9], and two DSE-based approaches [10]. The LSS(BBS) parameterization [7] assumes no quark orbital angular momentum, whereas quark orbital angular momentum is explicitly allowed in the Avakian *et al.* parameterization [8].

$$A_1^n = \frac{F_2^{^3\text{He}} \left[A_1^{^3\text{He}} - 2 \frac{F_2^p}{F_2^{^3\text{He}}} P_p A_1^p \left(1 - \frac{0.014}{2P_p} \right) \right]}{P_n F_2^n \left(1 + \frac{0.056}{P_n} \right)}. \quad (4)$$

The effective proton and neutron polarizations were taken as $P_p = -0.028^{+0.009}_{-0.004}$ and $P_n = 0.860^{+0.036}_{-0.020}$ [33]. F_2 was parameterized with F1F209 [24] for ^3He and with CJ12 [34] for the neutron and proton, while A_1^p was modeled with a Q^2 -independent, three-parameter fit to world data [1, 23, 35–39] on proton targets. Corrections were applied separately to the two beam energies, at the average measured Q^2 values of 2.59 (GeV/c) 2 ($E = 4.7$ GeV) and 3.67 (GeV/c) 2 ($E = 5.9$ GeV). The resulting neutron asymmetry, the statistics-weighted average of the asymmetries measured at the two beam energies, is given as a function of x in Table I and Fig. 1 and corresponds to an average Q^2 value of 3.078 (GeV/c) 2 . Table I also gives our results for the structure-function ratio $g_1^n/F_1^n = [y(1 + \epsilon R)]/[(1 - \epsilon)(2 - y)] \cdot [A_{\parallel} + \tan(\theta/2)A_{\perp}]$, where $y = (E - E')/E$ in the laboratory frame, which was extracted from our data in the same way as A_1^n with the same nuclear corrections.

Combining the neutron g_1/F_1 data with measurements on the proton allows a flavor decomposition to separate the polarized-to-unpolarized-PDF ratios for up and down quarks, which have a still greater ability than A_1^n to differentiate between various theoretical models. When the

TABLE I. A_1^n and g_1^n/F_1^n results.

$\langle x \rangle$	$A_1^n \pm \text{stat} \pm \text{syst}$	$g_1^n/F_1^n \pm \text{stat} \pm \text{syst}$
0.277	$0.043 \pm 0.060 \pm 0.020$	$0.044 \pm 0.058 \pm 0.012$
0.325	$-0.004 \pm 0.035 \pm 0.007$	$-0.002 \pm 0.033 \pm 0.009$
0.374	$0.078 \pm 0.029 \pm 0.010$	$0.053 \pm 0.028 \pm 0.010$
0.424	$-0.056 \pm 0.032 \pm 0.011$	$-0.060 \pm 0.030 \pm 0.013$
0.474	$-0.045 \pm 0.040 \pm 0.013$	$-0.053 \pm 0.037 \pm 0.016$
0.548	$0.116 \pm 0.072 \pm 0.018$	$0.110 \pm 0.067 \pm 0.019$

strangeness content of the nucleon is neglected, these ratios can be extracted at leading order as

$$\frac{\Delta u + \Delta \bar{u}}{u + \bar{u}} = \frac{4}{15} \frac{g_1^p}{F_1^p} (4 + R^{du}) - \frac{1}{15} \frac{g_1^n}{F_1^n} (1 + 4R^{du}) \quad (5)$$

$$\frac{\Delta d + \Delta \bar{d}}{d + \bar{d}} = \frac{4}{15} \frac{g_1^n}{F_1^n} (4 + \frac{1}{R^{du}}) - \frac{1}{15} \frac{g_1^p}{F_1^p} (1 + \frac{4}{R^{du}}) \quad (6)$$

where $R^{du} \equiv (d + \bar{d})/(u + \bar{u})$ and is taken from the CJ12 parameterization [34]; g_1^p/F_1^p was modeled with world data [1, 23, 35, 37–39] in the same way as A_1^p . Our results are given in Table II, and plotted in Fig. 2 along with previous world data and selected model predictions and parameterizations.

TABLE II. $\Delta u/u$ and $\Delta d/d$ results.

$\langle x \rangle$	$\Delta u/u \pm \text{stat} \pm \text{syst}$	$\Delta d/d \pm \text{stat} \pm \text{syst}$
0.277	$0.447 \pm 0.011 \pm 0.011$	$-0.166 \pm 0.094 \pm 0.023$
0.325	$0.505 \pm 0.006 \pm 0.010$	$-0.292 \pm 0.055 \pm 0.025$
0.374	$0.541 \pm 0.005 \pm 0.010$	$-0.252 \pm 0.048 \pm 0.028$
0.424	$0.600 \pm 0.005 \pm 0.011$	$-0.514 \pm 0.054 \pm 0.038$
0.474	$0.631 \pm 0.006 \pm 0.013$	$-0.579 \pm 0.070 \pm 0.052$
0.548	$0.642 \pm 0.009 \pm 0.019$	$-0.384 \pm 0.138 \pm 0.065$

Our results for A_1^n , $(\Delta u + \Delta \bar{u})/(u + \bar{u})$ and $(\Delta d + \Delta \bar{d})/(d + \bar{d})$ support previous measurements in the range $0.277 \leq x \leq 0.548$. The A_1^n data are consistent with a zero crossing between $x = 0.4$ and $x = 0.55$, as indicated by the JLab E99117 measurement [33]; a pQCD parameterization that explicitly permits quark orbital angular momentum [8] is a significantly better match to our data at large x than one that explicitly disallows it [7]. Our measurements of $(\Delta u + \Delta \bar{u})/(u + \bar{u})$ confirm the previously observed trend toward large positive values as x increases. Our results for $(\Delta d + \Delta \bar{d})/(d + \bar{d})$ show no evidence of a transition to a positive slope, as required by pQCD-based predictions, in the x range probed. While this result suggests that other models of nucleon structure in the high x regime may be fruitful, it is not yet

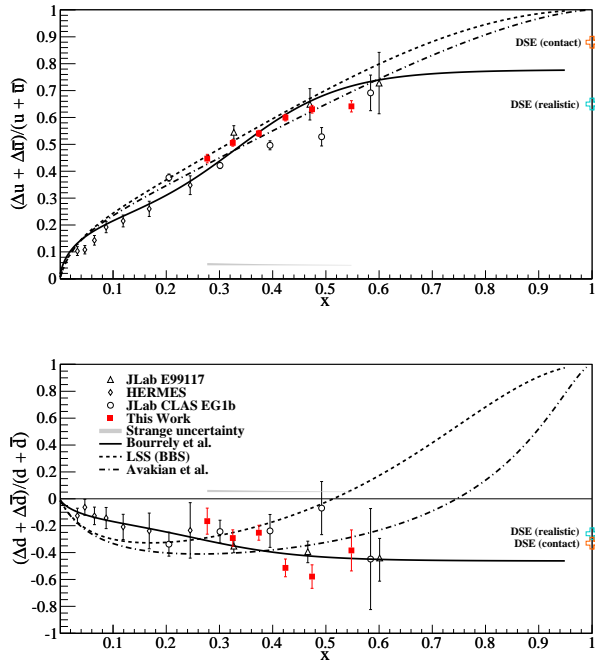


FIG. 2. Our results (red squares) for $(\Delta u + \Delta \bar{u})/(u + \bar{u})$ (top) and $(\Delta d + \Delta \bar{d})/(d + \bar{d})$ (bottom). The gray bands represent our estimated error from neglecting the strange-quark contribution. Also plotted are measurements from HERMES [37] (semi-inclusive DIS), JLab E99117 [33] (DIS), and JLab CLAS E91b [23] (DIS), in addition to predictions from the statistical model (Bourrely *et al.*) [9] and from two types of DSE-based approach [10]. The LSS(BBS) parameterization [7] assumes no quark orbital angular momentum, whereas quark orbital angular momentum is explicitly allowed in the Avakian *et al.* parameterization [8].

possible to reject any of the existing theoretical frameworks definitively. Our experimental setup differs significantly from those of previous measurements, relying on an open-geometry spectrometer deployed at a large scattering angle. With a gas Čerenkov detector and a pre-shower + shower calorimeter for particle identification, and with the ability to detect significant numbers of positrons even at the normal polarity setting, backgrounds due to π^- and to pair-produced electrons were sufficiently reduced that the measurement is a significant contribution to the world data set.

Two dedicated DIS A_1^n experiments [42, 43] have been approved to run at JLab in the coming years, pushing to higher x and studying the Q^2 evolution of the asymmetry. In advance of these experiments, and in combination with previous measurements, our data suggest that additional DIS measurements in the region $0.5 \leq x \leq 0.8$ will be of particular interest in establishing the high- x behavior of the nucleon spin structure; in addition, an extension of the DSE-based approach [10] to $x < 1$ would be valuable.

It is our hope that our data will inspire further theoretical work in the high- x DIS region.

We gratefully acknowledge the outstanding support of the Jefferson Lab Accelerator Division and Hall A staff in bringing this experiment to a successful conclusion. This work was supported in part by DOE grants DE-FG02-87ER40315 and DE-FG02-94ER40844. Jefferson Lab is operated by the Jefferson Science Associates, LLC, under DOE grant DE-AC05-06OR23177.

* dparno@uw.edu

† Deceased

- [1] J. Ashman *et al.* (EMC), Nucl. Phys. B **328**, 1 (1989).
- [2] C. A. Aidala *et al.*, Rev. Mod. Phys. **85**, 655 (2013).
- [3] D. de Florian *et al.*, Prog. Part. Nucl. Phys. **67**, 251 (2012).
- [4] N. Isgur, Phys. Rev. D **59**, 034013 (1999).
- [5] G. Farrar and D. R. Jackson, Phys. Rev. Lett. **35**, 1416 (1975).
- [6] G. Farrar, Phys. Lett. B **70**, 346 (1977).
- [7] E. Leader, A. V. Sidorov, and D. B. Stamenov, Int. J. Mod. Phys. A **13**, 5573 (1998).
- [8] H. Avakian *et al.*, Phys. Rev. Lett. **99**, 082001 (2007).
- [9] C. Bourrely, J. Soffer, and F. Buccella, Eur. J. Phys. C **23**, 487 (2002).
- [10] C. D. Roberts, R. J. Holt, and S. M. Schmidt, Phys. Lett. B **727**, 249 (2013).
- [11] W. Melnitchouk, R. Ent, and C. E. Keppel, Phys. Rep. **406**, 127 (2005).
- [12] K. Abe *et al.* (E143), Phys. Lett. B **452**, 194 (1999).
- [13] C. K. Sinclair *et al.*, Phys. Rev. Spec. Top. Accel. Beams **10**, 023501 (2007).
- [14] E. Babcock *et al.*, Phys. Rev. Lett. **91**, 123003 (2003).
- [15] J. Alcorn *et al.*, Nucl. Inst. Meth. A **522**, 294 (2004).
- [16] D. J. J. de Lange *et al.*, Nucl. Inst. Meth. A **406**, 182 (1998).
- [17] M. Posik, *A precision measurement of the neutron d_2 : Probing the color force*, Ph.D. thesis, Temple University (2014).
- [18] S. Escoffier *et al.*, Nucl. Inst. Meth. A **551**, 563 (2005).
- [19] M. Friend *et al.*, Nucl. Inst. Meth. A **676**, 96 (2012).
- [20] A. V. Glamazdin *et al.*, Fiz. B **8**, 91 (1999).
- [21] M. V. Romalis *et al.*, Nucl. Inst. Meth. A **402**, 260 (1998).
- [22] I. Kominis, *Measurement of the neutron (^3He) spin structure at low Q^2 and the extended Gerasimov-Drell-Hearn sum rule*, Ph.D. thesis, Princeton University (2001).
- [23] K. V. Dharmawardane *et al.* (CLAS), Phys. Lett. B **641**, 11 (2006).
- [24] P. E. Bosted and V. Mamyan, “Empirical fit to electron-nucleus scattering,” arXiv:1203.2262 [nucl-th].
- [25] A. Amroun *et al.*, Nucl. Phys. A **579**, 596 (1994).
- [26] L. W. Mo and Y. S. Tsai, Rev. Mod. Phys. **41**, 205 (1969).
- [27] I. Akushevich *et al.*, Comput. Phys. Commun. **104**, 201 (1997).
- [28] D. de Florian *et al.*, Phys. Rev. Lett. **101**, 072001 (2008).
- [29] D. Drechsel, S. S. Kamalov, and L. Tiator, Eur. Phys. J. A **34**, 69 (2007).
- [30] P. E. Bosted, Phys. Rev. C **51**, 409 (1995).
- [31] J. E. Amaro *et al.*, Phys. Rev. C **71**, 015501 (2005).

- [32] F. Bissey *et al.*, Phys. Rev. C **65**, 064317 (2002). 398
- [33] X. Zheng *et al.* (E99-117), Phys. Rev. C **70**, 065207 (2004). 399 400
- [34] J. F. Owens, A. Accardi, and W. Melnitchouk, Phys. Rev. D **87**, 094012 (2013). 401 402
- [35] J. Ashman *et al.* (EMC), Phys. Lett. B **206**, 364 (1988). 403
- [36] D. Adams *et al.* (SMC), Phys. Lett. B **336**, 125 (1994). 404
- [37] K. Ackerstaff *et al.* (HERMES), Phys. Lett. B **404**, 383 (1997). 405 406
- [38] K. Abe *et al.* (E143), Phys. Rev. D **58**, 112003 (1998). 407
- [39] P. L. Anthony *et al.* (E155), Phys. Lett. B **458**, 529 (1999). 408
- [40] P. L. Anthony *et al.* (E142), Phys. Rev. D **54**, 6620 (1996).
- [41] K. Abe *et al.* (E154), Phys. Rev. Lett. **79**, 26 (1997).
- [42] T. Averett *et al.*, “Measurement of neutron spin asymmetry A_1^n in the valence quark region using 8.8 GeV and 6.6 GeV beam energies and BigBite spectrometer in Hall A,” Jefferson Lab PAC 30 E12-06-122 (2006).
- [43] G. Cates *et al.*, “Measurement of neutron spin asymmetry A_1^n in the valence quark region using an 11 GeV beam and a polarized ^3He target in Hall C,” Jefferson Lab PAC 36, E12-06-110 (2010).